

Estimation of the time of exposure from the differential fading of luminescent detectors

Gianpaolo Roina^{1,*}, Debora Siqueira Nascimento^{1,2}, Riccardo Ciolini¹, Mariagrazia Quattrocchi³,
Francesco d'Errico^{1,4}

¹ School of Engineering, University of Pisa, Italy

² National Institute of Geophysics and Volcanology, Italy

³ S.C. Fisica Sanitaria Azienda Toscana Nord Ovest - Lucca, Italy

⁴ School of Public Health, Yale University, and Yale Center for Emergency Preparedness and Disaster Response, USA

(*) gianpaolo.roina@phd.unipi.it

Abstract— Containment and surveillance measures for unattended or remotely monitored items and areas serve to detect, timestamp, and thereby deter the illicit movement and trafficking of radioactive material in the interval between two successive inspections. This study explores the feasibility of a passive solution that does not rely on complex electronic components, thus mitigating common vulnerabilities of active instruments, including risks of tampering and unauthorised data access. The signal loss in luminescent materials – dependent on both time and temperature and previously investigated as a means of estimating the time of exposure – proved applicable in this safeguards-relevant context as well. The differential fading of peaks II and III of the glow curve of LiF:Mg,Cu,P (GR-200A), compared to the stable dosimetric peak IV, provided a means to timestamp the moment of irradiation with reasonable accuracy in the short- and medium-term after exposure. While the analysis primarily focused on the behaviour of individual crystals, the averaging of multiple responses was also explored for comparison, to assess its potential for reducing estimation error.

Keywords — differential fading; tamper-proof Chain of Custody verification; thermoluminescence; nuclear safeguards.

I. INTRODUCTION

TO verify that States are upholding their obligations under non-proliferation agreements, the International Atomic Energy Agency (IAEA) implements a range of safeguard measures, including scheduled on-site inspections. These inspections aim to validate the accuracy and completeness of declarations submitted by facility operators. A central concern in this context is ensuring the Continuity of Knowledge (CoK) on safeguarded items and areas between successive inspector visits. To address this need, the IAEA deploys dedicated optical surveillance systems and tamper-indicating seals that register access events, unauthorised movements of nuclear material, and any tampering with containment structures or Agency equipment, samples, and data.

Despite their effectiveness, these monitoring systems typically incorporate sophisticated electronic architectures,

which can present potential vulnerabilities to manipulation or covert interference. The present study explores the feasibility of a passive solution designed to detect the unauthorised removal of radioactive material from storage while also enabling retrospective estimation of the time at which such an event may have occurred. Additionally, application of the proposed approach to accidental radiation exposure scenarios might be possible, particularly in occupational settings, where accurate time reconstruction is essential for incident investigation and response.

The fading behaviour of luminescent materials under stimulation offers a promising method for estimating the time since exposure. While fading is typically regarded as a limitation in standard dosimetric practice, in this context it becomes an exploitable feature, offering a potential timestamping mechanism for radiation exposure events, particularly in scenarios relevant to nuclear safeguards and traceability. Early work in this direction – albeit aimed at dosimetric applications – was proposed by Moscovitch [1], who developed an automated method for estimating the elapsed time between irradiation and readout in LiF:Mg,Ti by analysing the fading behaviour of individual glow peaks. More recently, d'Errico et al. [2] extended this concept to safeguards-related scenarios, demonstrating the feasibility of estimating the time of exposure by comparing the fading signals of various luminescent materials. Building on this approach, our study advanced the concept by relying on a single material – LiF:Mg,Cu,P (GR-200A) – to obtain similar information, correlating the time elapsed since exposure with the fading of specific peaks in its thermoluminescent glow curve. The level of timestamping accuracy achieved with this method is discussed later in the paper.

The fading at room temperature of these peaks has been previously studied by Budzanowski et al. [3], who confirmed their exponential behaviour and the potential to estimate the time of exposure by examining the peak II-to-IV and III-to-IV area ratios. This methodology has been successfully applied in personal and environmental dosimetry to reconstruct the timing of high-dose-rate accidental exposures, with results that closely matched actual exposure times [4], validating the practicality of the approach.

While a more detailed discussion of the theoretical aspects of this research will be reported in a future publication, the present work offers an overview of the principal results.

II. MATERIALS AND METHODS

This work used LiF:Mg,Cu,P-based thermoluminescent detectors (GR-200A), selected for their high sensitivity and suitability for low-dose applications. They are manufactured in disc form with a diameter of 4.5 mm and a thickness of 0.8 mm. The luminescence spectrum closely resembles that of LiF:Mg,Ti (TLD-100) [5], and the linearity of the dose response is maintained up to roughly 1 Gy [6], making it appropriate for the dose range under investigation.

LiF:Mg,Cu,P typically shows six glow peaks between 90 °C and 350 °C, but the short half-life of peak I limits its practical use, while peaks V and VI require reading temperatures above 240 °C, which can potentially affect crystal structure. Therefore, only peaks II, III, and IV were considered, with the latter used as a reference due to its relative insensitivity to post-irradiation fading. In contrast, peaks II and III undergo progressive signal loss over time, with markedly different decay rates – approximately one day and three months, respectively [7]. These differing stability characteristics enable time-resolved analysis of the luminescent response.

As a preliminary step, an initial set of 146 crystals was examined to identify the largest possible group of highly homogeneous crystals presenting the same response ($\pm 5\%$) to a given dose of 1 mGy. They were irradiated at the Nuclear Measurements Laboratory of the University of Pisa (Italy) – School of Engineering, using a 2.22 MBq Ra-226 radioactive source placed on top of a specially designed Plexiglas apparatus. The mass of each crystal was also accurately measured with an ABT 100-5NM KERN[®] analytical balance (readability of 0.01 mg), to relate the total and peak-specific generated charges to the unit mass of the phosphor, as mass ultimately influences the thermoluminescent light emitted for a given absorbed dose.

The 88 identified homogenous crystals were irradiated using a 6 MV photon beam from a medical linear accelerator at San Luca Hospital in Lucca (Italy), delivering a dose of 100 mGy (10 monitor units) over 6 seconds at the lowest available dose rate. Notably, the short duration of the irradiation resembles real-world scenarios in which a perpetrator carrying a stolen source would move swiftly past the detection system, resulting in only brief exposure times. A 1.5 cm solid water build-up layer was placed above the samples, with an additional 15 cm beneath them to ensure full backscatter conditions. To reconstruct the fading curves over the first week and the two months after exposure, numerous irradiation–readout cycles had to be performed, and permutation of the crystal readout order at each cycle ensured adequate temporal sampling of the individual elements during both intervals.

A Harshaw 4500 Manual TLD Reader operated via the WinREMS interface acquired the thermoluminescence signal under nitrogen flow using a resistive heating system that delivered a linear temperature profile from 40 °C to 240 °C over 200 seconds. Indeed, the adoption of the lowest available heating rate enhanced the resolution between peak III and the

low-temperature tail of peak IV. Each readout produced a 200-point glow curve with peak maxima at approximately 110, 160, and 210 °C. A 10-second annealing phase at 240 °C followed the data acquisition, resulting in a residual signal below 2% of the measured value.

The software GlowFit v1.3 [8] was used to decompose the experimental glow curves into individual peaks using a first-order kinetic model with a linear heating profile. Initial estimates of the three kinetic parameters E , T_m and I_m (trap depth, and temperature and intensity of the maximum) associated with each peak are iteratively adjusted via the Levenberg–Marquardt algorithm to minimise the χ^2 error between the experimental and fitted curves.

Finally, a custom MATLAB script was used to process the glow-curve experimental data and the associated kinetic parameters to analyse the specifics of the three peaks, particularly the ratios between the areas underneath. The results are discussed in the following section.

III. RESULTS AND DISCUSSION

The temporal variation of the peak II-to-IV and III-to-IV area ratios generated the fading curves required for the intended safeguards-related application. In the envisioned scenario, an inspector suspecting the illicit removal of nuclear material would be able to estimate the time t_{est} potentially elapsed since the removal by comparing the peak area ratios calculated from the crystal readouts with those reported in Fig. 1.

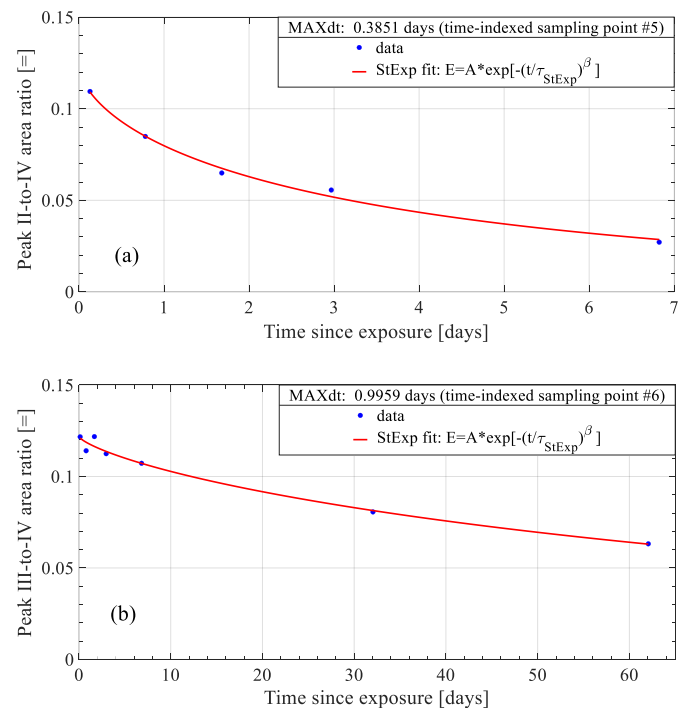


Fig. 1 Variation of the peak II-to-IV (a) and III-to-IV (b) area ratios with time after exposure for one of the crystals used in the study (illustrative example), showing experimental data and stretched exponential fit.

In mathematical terms, we introduced the fitting function

$$PAR^{X/IV} = f(t) \quad (1)$$

that approximates the experimental data points

$$\left(t_i, \text{PAR}_i^{\text{X/IV}} \right) \quad \forall i \quad (2)$$

for the generic peak X-to-IV area ratio ($X = \text{II}$ or III). Its inverse, $t = f^{-1}(\text{PAR}^{\text{X/IV}})$, allows estimation of t_{est} from the measured ratio:

$$t_{\text{est}} = f^{-1} \left(\text{PAR}_{\text{meas}}^{\text{X/IV}} \right). \quad (3)$$

The overall data pattern exhibited exponential-like behaviour, as expected. However, a ‘‘stretched exponential relaxation’’ model [9] was preferred to the simpler one-term exponential decay due to its ability to capture the long-time fading tail of the experimental data (Fig. 2). This is attributable to the characteristic $t^{\beta-1}$ decrease in the decay rate $1/\tau_{\text{StExp}}$, that causes the graph of $\ln(f_{\text{StExp}})$ to exhibit a characteristic stretch when $0 < \beta < 1$:

$$f_{\text{StExp}}(t) = A \cdot \exp \left[- \left(\frac{t}{\tau_{\text{StExp}}} \right)^\beta \right] \quad (\beta > 0) \quad (4)$$

Such behaviour can be explained as a linear superposition of simple exponential decays (note that $f_{\text{StExp}}(t)$ becomes exponential for a unit value of β), and it was already used by Werner [10] to describe complex luminescence decays.

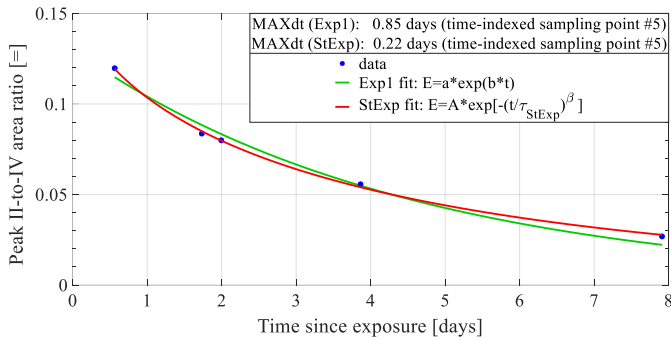


Fig. 2 Comparison of stretched exponential (red) and one-term exponential (green) fits to peak II-to-IV area ratios as a function of time since exposure in the single-crystal approach.

In order to compare various fitting models, as well as to quantify the accuracy of the time estimation, we defined the ‘‘maximum horizontal distance’’, MAXdt, as the largest of the absolute differences between the experimental fading times, t_i , and the values of the inverse function evaluated at the corresponding experimental peak area ratios $\text{PAR}_i^{\text{X/IV}}$ (what is referred to as the i -th ‘‘horizontal distance’’, Δt_i):

$$\text{MAXdt} = \max_i \{ \Delta t_i \} = \max_i \left\{ \left| t_i - f^{-1} \left(\text{PAR}_i^{\text{X/IV}} \right) \right| \right\}. \quad (5)$$

Confirming prior considerations, for the vast majority ($\sim 90\%$) of the analysed crystals the value of MAXdt calculated using a stretched exponential relaxation was smaller than that corresponding to the one-term exponential model, indicating a

better fit. Additional goodness-of-fit parameters were also evaluated (Table I) and further corroborated these results.

TABLE I
COMPARISON OF GOODNESS-OF-FIT PARAMETERS OF FITTING MODELS

| GoF parameter | Ideal parameter value | Stretched exponential fit | One-term exponential fit |
|---------------|-------------------------|---------------------------|--------------------------|
| SSE | SSE $\rightarrow 0$ | 1.987e-5 | 1.17e-4 |
| R-square | $R^2 \rightarrow 1$ | 0.99602 | 0.9767 |
| Adj. R-square | Adj $R^2 \rightarrow 1$ | 0.99205 | 0.96894 |
| RMSE | RMSE $\rightarrow 0$ | 0.0031513 | 0.0062277 |

SSE = Sum of Squares Due to Error; Adj. R-square = Degrees of Freedom Adjusted R-Square; RMSE = Root Mean Squared Error.

To extend the evaluation of our model performance, a statistical analysis of the estimation accuracy of the stretched exponential model was conducted for all crystals and both peak area ratios. The outcomes are presented in Figs. 3a and 4a as histograms illustrating the distribution of the maximum absolute differences between the experimental data and the fit. The corresponding cumulative percentage curves were superimposed to offer a comprehensive overview of the accuracy performance across the dataset.

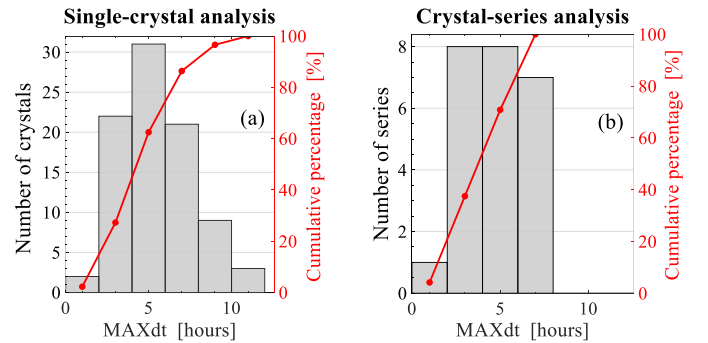


Fig. 3 Accuracy in estimating the time elapsed after exposure from peak II-to-IV area ratios for the single-crystal (a) and the crystal-series (b) approaches.

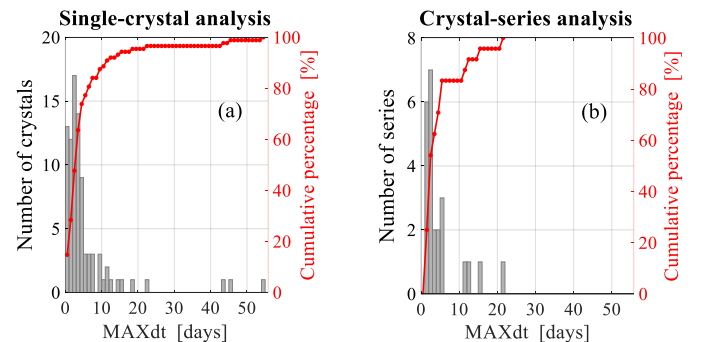


Fig. 4 Accuracy in estimating the time elapsed after exposure from peak III-to-IV area ratios for the single-crystal (a) and the crystal-series (b) approaches.

In the first week after exposure, the peak II-to-IV area ratio yielded an estimated exposure time of 8 hours or less from the actual event for 86% of the analysed crystals. A comparable

result was observed over the first two months, with the peak III-to-IV area ratio achieving a deviation of less than 5 days in 74% of cases.

A similar analysis is shown in Figs. 5a and 6a, illustrating how the time-indexed sampling points with the lowest accuracy in the individual fading curves were spread across all crystals. As expected, for both peak area ratios accuracy dropped at longer fading times, as the decomposition software and the fitting model become less capable of capturing the disappearing low-temperature peaks. A comparable decline in accuracy was also observed for the peak II-to-IV area ratio at short fading times, where peak II shows the greatest variation.

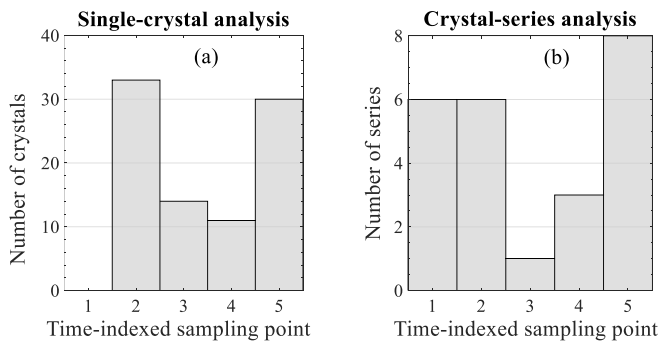


Fig. 5 Distribution of lowest-accuracy time-indexed sampling points for peak II-to-IV area ratios in the single-crystal (a) and the crystal-series (b) approaches.

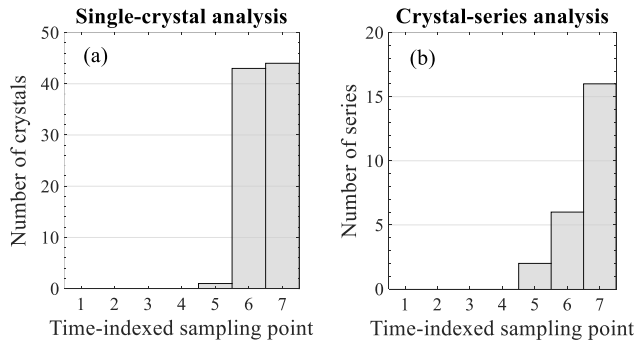


Fig. 6 Distribution of lowest-accuracy time-indexed sampling points for peak III-to-IV area ratios in the single-crystal (a) and the crystal-series (b) approaches.

While prioritising the analysis of individual crystal behaviours, we also examined the fading curves derived from series-averaged data. This complementary approach builds on the initial crystal selection process (see Materials and Methods), where groups of crystals with comparable responses were identified, and was explored solely for comparative purposes, to assess whether averaging could enhance the accuracy of the results. A total of 24 series were considered, each comprising a variable number of crystals. At each time sampling point, the measured peak area ratios of the crystals within a given series were averaged, and the resulting values were then fitted using the same stretched exponential model to produce the corresponding fading curve (Figs. 7-9).

To facilitate comparison of overall estimation accuracy across the full dataset, similar histograms with superimposed cumulative percentage curves were generated (Figs. 3b, 4b, 5b, 6b).

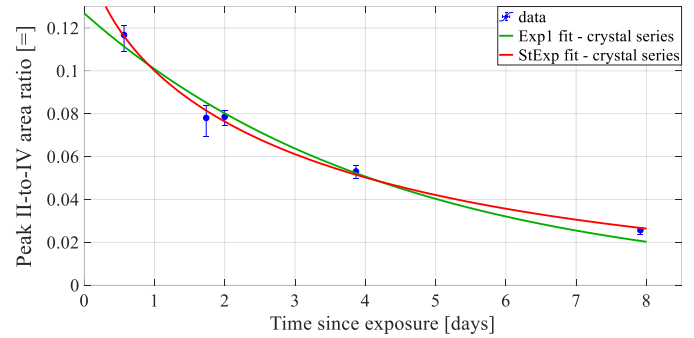


Fig. 7 Comparison of stretched exponential (red) and one-term exponential (green) fits to peak II-to-IV area ratios as a function of time since exposure in the crystal-series approach.

The series-based approach seems to produce slightly more accurate results in both intervals of interest, indicating that averaging may help reduce part of the inherent variability in the data. This is further supported by a numerical comparison of MAXdt values, which shows that, in just over half of the cases, the series-averaged method results in a lower estimation error. It is also worth mentioning that, in general, the maximum deviation for each series s tends to approximate the arithmetic mean of the MAXdt values of the N_s crystals composing it:

$$\text{MAXdt}_s \approx \frac{1}{N_s} \sum_{i=1}^{N_s} \text{MAXdt}_{i,s} \quad \forall s. \quad (6)$$

IV. CONCLUSIONS

This study evaluated the effectiveness of a passive method for detecting the unauthorised removal of radioactive material from storage, with the added capability of retrospectively estimating the time of the event. Building on previous research that connected time- and temperature-dependent signal loss in luminescent materials to post-exposure timing, the approach was expanded into a single-material framework (LiF:Mg,Cu,P) by relating the time factor to the differential fading of its low-temperature glow peaks. Fitting a stretched exponential model to the evolution of peak II-to-IV and III-to-IV area ratios in the individual fading behaviour of each analysed crystal has demonstrated the capacity to estimate the precise timing of the event within a margin of a few hours to a few days over the first week and two months after exposure. These estimates can be further refined, to some degree, by averaging signals from multiple crystals with similar responses. Since the half-life of the glow peaks influences the system's effectiveness, current research is investigating alternative luminescent materials with longer-lived peaks to broaden their applicability to applications featuring longer intervals between inspections.

REFERENCES

- [1] M. Moscovitch, "Automatic method for evaluating elapsed time between irradiation and readout in LiF-TLD", *Radiat. Prot. Dosim.*, vol. 17, no. 1-4, pp. 165-169, Dec. 1986, 10.1093/rpd/17.1-4.165.
- [2] F. d'Errico, D. O. Junot, I. O. Polo, A. Chierici, R. Ciolini, D. N. Souza, et al., "Differential-fading optically stimulable materials for Nuclear Safeguards", in *Proc. INAC 2019*, Santos, SP, Brazil, 2019, pp. 3838-3843.

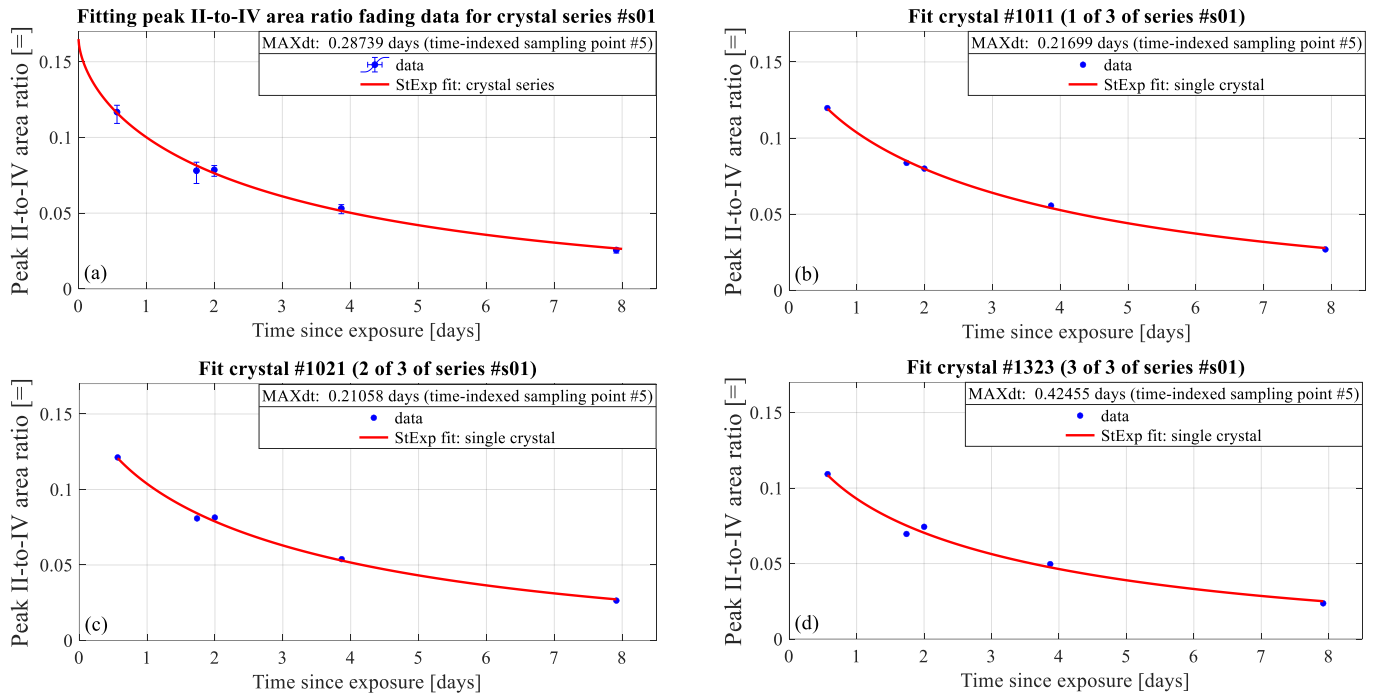


Fig. 8 Comparison of fading curves of peak II-to-IV area ratios versus time after exposure for a crystal series (a) and the individual crystals composing it (b–d). All data were fitted using a stretched exponential model.

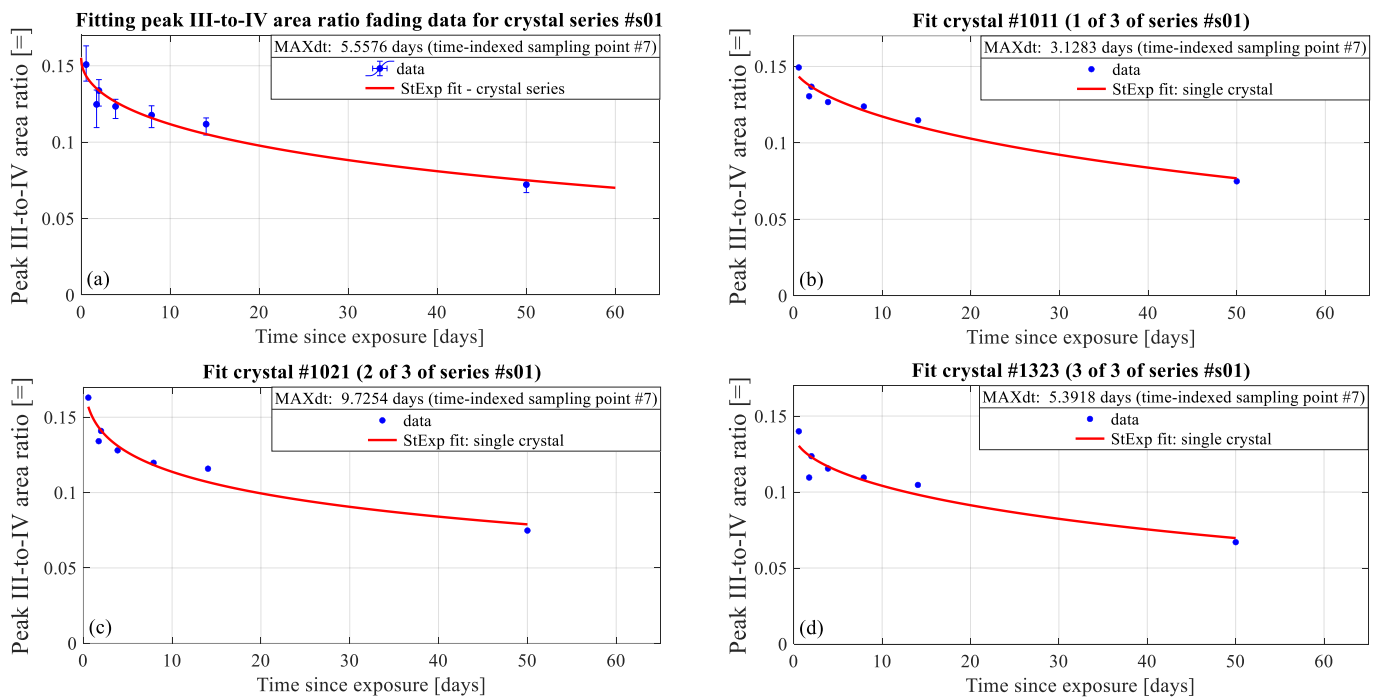


Fig. 9 Comparison of fading curves of peak III-to-IV area ratios versus time after exposure for a crystal series (a) and the individual crystals composing it (b–d). All data were fitted using a stretched exponential model.

- [3] M. Budzanowski, J. C. Sáez-Vergara, J. M. Gómez-Ros, A. Romero, E. Ryba, “The fading of different peaks in LiF:Mg,Cu,P (MCP-N and GR-200A) TL detectors”, *Radiat. Meas.*, vol. 29, no. 3–4, pp. 361–364, May 1998, 10.1016/S1350-4487(98)00028-6.
- [4] M. Budzanowski, J. C. Sáez-Vergara, E. Ryba, P. Bilski, P. Olko, M. P. R. Waligórski, “Estimation of the time elapsed between exposure and readout using peak ratios of LiF:Mg,Cu,P (MCP-N, GR200A)”, *Radiat. Prot. Dosim.*, vol. 85, no. 1, pp. 149–152, Sep. 1999, 10.1093/oxfordjournals.rpd.a032822.
- [5] L. A. DeWerd, J. R. Cameron, W. Da-Ke, T. Papini, I. J. Das, “Characteristics of a new dosimeter material: LiF(Mg,Cu,P)”, *Radiat. Prot. Dosim.*, vol. 6, no. 1–4, pp. 350–352, Dec. 1983, 10.1093/oxfordjournals.rpd.a082948.

- [6] G. F. Knoll, “Miscellaneous detector types” in *Radiation Detection and Measurement*, 4th ed., Hoboken, NJ, USA: Wiley, 2010, ch. 19, sec. VII, pp. 755-757.
- [7] E. Martella, “Dosimetric characteristics of LiF:Mg,Cu,P (GR-200A)”, ASG–S.R.L., Italy, 1993. [Online] Available: <https://www.mc2dna.com/wp-content/uploads/gr-200a.pdf>.
- [8] M. Puchalska, P. Bilski, “GlowFit—a new tool for thermoluminescence glow-curve deconvolution”, *Radiat. Meas.*, vol. 41, no. 6, pp. 659–664, Jul. 2006, 10.1016/j.radmeas.2006.03.008.
- [9] D. C. Elton, “Stretched exponential relaxation,” *arXiv [cond-mat.dis-nn]*, Aug. 2018, 10.48550/arXiv.1808.00881.
- [10] A. Werner, 1907, “Quantitative messungen der an- und abklingung getrennter phosphoreszenzbanden”, *Ann. Phys.*, vol. 329, no. 11, pp. 164-190, Aug. 1907, 10.1002/andp.19073291111.